JGR Atmospheres

RESEARCH ARTICLE
10.1029/2022JD037218

Key Points:

- Atmospheric anomaly signals can persist from zero to several months in the form of soil temperature (ST) anomalies in shallow soil
- The reemergence of ST anomalies in shallow soil from air temperature is a more common phenomenon than the one from precipitation
- Freeze-thaw process is one of the processes that lead to the reemergence of ST anomalies

Supporting Information:

Supporting Information may be found in the online version of this article.

Correspondence to:

Y. Song, A. Huang, and H. Chen,
songym@nuist.edu.cn;
anhuang@nju.edu.cn;
haishan@nuist.edu.cn

Citation:

Song, Y., Huang, A., & Chen, H. (2022). The persistence and reemergence of atmospheric anomaly signals in soil temperature. *Journal of Geophysical Research: Atmospheres*, *127*, e2022JD037218. https://doi.org/10.1029/2022JD037218

Received 31 MAY 2022
Accepted 15 SEP 2022

Author Contributions:

Conceptualization: Yaoming Song
Data curation: Yaoming Song, Anning Huang
Formal analysis: Yaoming Song, Anning Huang
Funding acquisition: Yaoming Song, Anning Huang, Haishan Chen
Investigation: Yaoming Song, Haishan Chen
Methodology: Yaoming Song
Project Administration: Anning Huang
Resources: Yaoming Song, Haishan Chen
Software: Yaoming Song
Supervision: Anning Huang, Haishan Chen
Validation: Yaoming Song, Anning Huang
Visualization: Yaoming Song, Anning Huang, Haishan Chen

The Persistence and Reemergence of Atmospheric Anomaly Signals in Soil Temperature

Yaoming Song[1,2], Anning Huang[3], and Haishan Chen[1,2]

[1]Collaborative Innovation Center on Forecast and Evaluation of Meteorological Disasters(CIC-FEMD), Nanjing University of Information Science & Technology, Nanjing, China, [2]School of Atmospheric Sciences, Nanjing University of Information Science & Technology, Nanjing, China, [3]School of Atmospheric Sciences, Nanjing University, Nanjing, China

Abstract The anomalies of soil temperature (ST) in shallow soil are potential signals for both weather forecast and climate prediction. Results show atmospheric anomaly signals can persist from zero to several months in the form of ST anomalies in shallow soil, and the persistence of ST anomalies caused by atmospheric anomalies in different months is significantly different. ST anomalies in shallow soil caused by air temperature can persist for longer time than those caused by precipitation. The decrease in instantaneous precipitation and air temperature leads to the weakening of atmosphere interference with ST anomaly persistence, which enhances the persistence of ST anomalies caused by initial air temperature anomalies. Moreover, the reemergence of ST anomalies in shallow soil from air temperature is a more common phenomenon than one from precipitation. ST anomaly reemergence may be caused by two processes. Freeze-thaw process is one of the processes, and it has been confirmed in both observations and simulations. Another may be related to the changes of the vertical distributions of hydraulic and thermal conductivities due to the changes in air temperature and precipitation when the climate shifts from warm-wet to cold-dry. However, the reemergence of ST anomalies only occurs in the simulations where freeze-thaw processes exist using the Community Land Model 4.5 (CLM4.5). The persistence and reemergence of observed ST anomalies are not fully captured in numerical simulations using CLM4.5, which requires further research to improve the simulation performance of numerical models.

1. Introduction

Land surface is one of the important components of the earth climate system, and soil temperature (ST) is a key factor of land surface processes. As an indicator of heat storage in land surface, ST plays an important role in land-atmosphere interactions. The anomalies in ST can change surface sensible flux, latent flux, longwave radiation, etc., and further affect weather and climate on multiple time scales (Q. Hu & Feng, 2004; Mahanama et al., 2008; Wu & Zhang, 2014). Moreover, ST can change the locations and intensities of precipitation by affecting the development of convection (Fan, 2009; Y. Liu & Avissar, 1999; Xue et al., 2018), and also facilitates the occurrence of the extreme heat events by local land-atmosphere coupling and changing atmospheric circulation (Gómez et al., 2016).

The anomalies of ST usually depend on atmospheric anomalies, which are resulted from the anomalous sea surface temperature and sea ice, etc., and then ST anomalies can affect subsequent atmosphere by the persistence of the anomalies. For example, anomalous ST in winter can affect the precipitation in following spring (Tang et al., 1987), and ST in late spring correlates well with summer precipitation (Mahanama et al., 2008). Y. H. Wang et al. (2013) revealed that ST in May over Northwest China can affect summer precipitation by changing the East Asian summer monsoon. Ma (1995) found that there is a close relationship between antecedent ST anomalies and the subsequent floods in the Yangtze–Huaihe River Basin. Xue et al. (2018) demonstrated that spring land surface and subsurface temperature anomalies have important effects on the subsequent downstream droughts/floods in late spring-summer over North America and East Asia.

The relationship between ST and subsequent atmosphere depends on the persistence of antecedent ST anomalies, which is also known as ST memory. ST anomalies can persist for a period ranging from 1 month to years, with the dependence of season, soil depth and climate regime, etc (Y. Liu & Avissar, 1999; K. Yang & Zhang, 2016). For example, in cold regions, ST anomalies in autumn can be stored in the frozen soil during the winter, and then reappear at the surface during the thaw (Matsumura & Yamazaki, 2012; Schaefer et al., 2007). The changes of ST

Writing – original draft: Yaoming Song
Writing – review & editing: Yaoming Song, Anning Huang, Haishan Chen

depend on radiation, air temperature (Kang et al., 2000; H. X. Zhang et al., 2021), precipitation (García-Suárez & Butler, 2006), vegetation cover types (H. Hu et al., 2009; Tesař et al., 2008; S. Y. Zhang & Li, 2018), soil physical properties (Ceccon et al., 2011), wind speed (Mihalakakou et al., 1997), topography changes (Wundram et al., 2010) and snow (Iijima et al., 2010; Qian et al., 2011). Among all factors affecting ST, air temperature and precipitation are the two most important factors (Helama et al., 2011; Y. Yang et al., 2018). Chen et al. (2020) found that the deep ST is closely correlated with air temperature. H. X. Zhang et al. (2021) revealed that the ST anomalies caused by air temperature anomalies can propagate downward to the deep soil layer after several months. Song et al. (2022) showed that both the storage of air temperature signals in deep ST even after 4 months and the storage of precipitation signals in shallow ST after 1 month are widespread phenomena in China.

Driven by the atmospheric forcing, ST anomalies occur, and then anomaly signals can be stored in ST for a period of time. Generally, ST anomalies can affect subsequent atmosphere when persistent anomalies are stored in shallow soil layers, or can propagate from deep to shallow soil, or are stored in other form and then cause later ST anomalies. The phenomenon of disappearance and reappearance of anomaly signals in shallow soil is called reemergence of anomaly signals. Many studies have demonstrated that the anomalies of ST can persist, but there is a lack of understanding of how ST anomalies persist and the persistent feature of ST anomalies. How long can ST anomalies persist in shallow soil layers? Can the ST anomaly signals propagated to deep soil be able to propagate to shallow soil after a certain period of time, making it possible to affect subsequent atmosphere? The influence of atmospheric conditions on the characteristics of the persistence of ST anomalies also remains unclear. The main aim of this study is to try to understand the persistence of ST anomalies caused by atmospheric anomalies and the effect of atmospheric conditions on anomaly persistence both in the observations and land surface simulations. In addition, the physical processes related to ST anomaly persistence need further investigated. In this study, air temperature and precipitation, two main variables affecting ST among atmospheric variables, are mainly considered (Helama et al., 2011; Y. Yang et al., 2018).

2. Data, Methods, Model, and Experimental Design

2.1. Data

The observed monthly data is provided by the China Meteorological Administration, which includes air temperature (1.5 m), monthly precipitation and ST at the seven soil layers of 5, 10, 20, 40, 80, 160, and 320 cm from 1960 to 2013. To reduce the effect of missing values in ST data, we adopted seven sites with as few missing data as possible at seven soil layers from 1960 to 2013, and the seven sites include Wuhan (114°10'E, 30°15'N), Tianshui (105°20'E, 34°21'N), Kunming (102°26'E, 25°01'N), Lhasa (91°01'E, 29°26'N), Beijing (116°12'E, 39°34'N), Lanzhou (103°34'E, 36°02'N) and Harbin (126°23'E, 45°27'N). The locations of the seven sites can refer to the paper of Song et al. (2022). Moreover, we used the 30 min interval data including precipitation, 2 m temperature and ST observed at Tongyu site (122°52'E, 44°25'N) in 2004 to drive the land surface model to simulate the response of land surface variables to precipitation and air temperature anomalies. The vegetation type is grass at Tongyu site. In addition, the water table depth is set to 9 m. Based on the soil texture data in the CLM4.5, the sand, clay, and organic matter in soil are about 70%, 5%, and 25%, which are different with soil depths at Tongyu site.

2.2. Methods

The effects of antecedent precipitation and air temperature on ST are represented by lag correlation, and the effects also can be considered as the storage and propagation of atmospheric anomaly signals in ST. The lag correlation coefficients between antecedent air temperature or precipitation in 12 months and ST with lag of 0–12 months at seven sites are obtained. The persistence and reappearance of anomaly signals in shallow soil are shown by the correlations between atmospheric anomalies and subsequent ST in shallow soil. Empirical orthogonal function (EOF) is used to decompose the lag correlation coefficients to get the common characteristics of the storage and propagation of the signals of atmospheric anomaly in the ST at different soil depths with increasing lag time. Upward propagation of antecedent downward propagating anomaly signals in soil is one of the important processes leading to ST anomaly reemergence, including the downward propagation of atmospheric anomaly signals, the storage of anomaly signals in soil and upward propagation of the stored anomaly signals. ST anomaly signals can be stored in the form of soil freezing, and ST anomaly signals reap-

pear when soil thaws, which also can cause ST anomaly reemergence. In order to determine the months in which ST anomalies caused by atmospheric anomalies can reemerge after a period of time at the seven sites, ideal anomaly signal propagation pattern are established, which include the downward propagation, storage, and upward propagation of anomaly signals. The ideal patterns can be adjusted with several parameters, and the correlation coefficient between the ideal patterns and the propagation pattern of ST anomaly signals is used to determine whether ST anomaly reemergence is likely to occur. At the seven sites, the months in which ST anomalies caused by atmospheric anomalies can reemerge after a period of time are selected to analyze the correlation coefficients between air temperature/precipitation in initial months (TIM/PIM) and subsequent ST (C-TIM-ST, C-PIM-ST), and the data in the first month is used as TIM/PIM. Based on the stepwise regression analysis on the relationships between ST at a certain depth in a certain month and air temperature/precipitation with the lead time of 0–12 months, the corresponding time of air temperature/precipitation which is closely related to the variation of the ST at the certain depth in the certain month are obtained. Moreover, we calculate the correlation coefficients between TIM/PIM and subsequent air temperature/precipitation, and calculate the monthly climatology of air temperature, precipitation, and ST in 12 months of a year. And then, combined with the results of stepwise regression analysis, the factors affecting signal propagation are analyzed. In addition, the accumulations of air temperature/precipitation between the month corresponding to TIM/PIM and the month of ST are calculated, which are named as T-climate and P-climate, respectively. The correlation coefficients between the accumulations of air temperature/precipitation and C-TIM-ST/C-PIM-ST are calculated to represent the effects of the climate conditions on C-TIM-ST/C-PIM-ST. The correlation coefficients between TIM/PIM and C-TIM-ST/C-PIM-ST are also calculated to reveal the effect of the degree of TIM/PIM anomalies (D-TIM-A/D-PIM-A) on C-TIM-ST/C-PIM-ST.

2.3. Model Description

In this study, the Community Land Model version 4.5 (CLM4.5) is used to study the response of land surface variables to air temperature/precipitation anomalies. The CLM4.5 can reproduce well the land surface variables including water and heat flux, ST, soil moisture, etc (Brunke et al., 2016; Guo et al., 2018; D. Liu & Mishra, 2017; Song et al., 2014; A. Wang et al., 2016). The CLM4.5 is developed as the land surface component of the Community Earth System Model in the National Center of Atmospheric Research (Oleson et al., 2013). It includes the terrestrial biogeophysical and biogeochemical processes related to land-atmosphere interactions.

2.4. Experimental Design

To study the response of land surface variables to different atmospheric anomalies in different atmospheric conditions, 10 sets of simulation experiments are carried out using CLM4.5, corresponding to 10 atmospheric conditions. The first nine experiments in Table 1 include one control experiment and four sensitivity experiments, and sensitivity experiments include dry/wet precipitation anomalies and cold/warm air temperature anomalies in the first month of the numerical experiments. Our pre-research and some literatures suggest that freeze-thaw process may have important effect on the storage and propagation of ST anomaly signals in soil (Matsumura & Yamazaki, 2012; Schaefer et al., 2007); therefore, FT experiments are designed with a period of time when air temperature is below 0°C. In FT experiments, one control and two sensitivity experiments with wet and warm atmospheric anomalies are performed. The first month in the numerical experiments is also called the initial month. The atmospheric variables in the experiments are based on the observations at Tongyu in 2003 and 2004. The total annual precipitation is 308 mm, and the average annual temperature is 9.09°C at Tongyu in 2003 and 2004. And all experiments have the same initial vertical soil moisture and ST profile. The dry and wet conditions are built using the observed precipitation data multiplied by 0.5 and 2, respectively; similarly, the warm and cold conditions are built using the observed temperature data plus and minus 10°C, respectively. All experiments described above are summarized in Table 1. Moreover, the correlation coefficient between temperature/precipitation and relative humidity is 0.95/0.71 at the seven sites, which shows that relative humidity have a strong dependence on temperature and precipitation. The changes of air temperature and precipitation in the atmospheric forcing data used in CLM4.5 may require consideration of corresponding changes of relative humidity, which is more consistent with the characteristics of the real atmosphere. Therefore each numerical experiment is performed under two atmospheric conditions, one in which relative humidity varies with temperature/precipitation and another in which relative humidity does not vary with temperature/precipitation.

Table 1
Design of the Experiments for Different Atmospheric Anomalies in the First Month and Different Atmospheric Conditions

		Precipitation anomaly in initial month	Air temperature anomaly in initial month	Precipitation	Temperature
T1R05	Control	0	0	Observed × 0.5	Observed
	Cold anomaly	0	−5°C		
	Warm anomaly	0	+5°C		
	Wet anomaly	Observed × 2.0	0		
	Dry anomaly	Observed × 0.5	0		
T1R1	Control	0	0	Observed	Observed
	Cold anomaly	0	−5°C		
	Warm anomaly	0	+5°C		
	Wet anomaly	Observed × 2.0	0		
	Dry anomaly	Observed × 0.5	0		
T1R2	Control	0	0	Observed × 2	Observed
	Cold anomaly	0	−5°C		
	Warm anomaly	0	+5°C		
	Wet anomaly	Observed × 2.0	0		
	Dry anomaly	Observed × 0.5	0		
T2R05	Control	0	0	Observed × 0.5	Observed + 10°C
	Cold anomaly	0	−5°C		
	Warm anomaly	0	+5°C		
	Wet anomaly	Observed × 2.0	0		
	Dry anomaly	Observed × 0.5	0		
T2R1	Control	0	0	Observed	Observed + 10°C
	Cold anomaly	0	−5°C		
	Warm anomaly	0	+5°C		
	Wet anomaly	Observed × 2.0	0		
	Dry anomaly	Observed × 0.5	0		
T2R2	Control	0	0	Observed × 2	Observed + 10°C
	Cold anomaly	0	−5°C		
	Warm anomaly	0	+5°C		
	Wet anomaly	Observed × 2.0	0		
	Dry anomaly	Observed × 0.5	0		
T05R05	Control	0	0	Observed × 0.5	Observed − 10°C
	Cold anomaly	0	−5°C		
	Warm anomaly	0	+5°C		
	Wet anomaly	Observed × 2.0	0		
	Dry anomaly	Observed × 0.5	0		
T05R1	Control	0	0	Observed	Observed − 10°C
	Cold anomaly	0	−5°C		
	Warm anomaly	0	+5°C		
	Wet anomaly	Observed × 2.0	0		
	Dry anomaly	Observed × 0.5	0		

Table 1
Continued

		Precipitation anomaly in initial month	Air temperature anomaly in initial month	Precipitation	Temperature
T05R2	Control	0	0	Observed × 2	Observed − 10°C
	Cold anomaly	0	−5°C		
	Warm anomaly	0	+5°C		
	Wet anomaly	Observed × 2.0	0		
	Dry anomaly	Observed × 0.5	0		
FT	Control	0	0	Observed	Observed − 10°C in the 2nd to 9th months; observed in other
	Warm anomaly	0	+5°C		
	Wet anomaly	Observed × 2.0	0		

Note. "Observed" in the table is based on the observation at TongYu site in 2003 and 2004. Warm, Cold, Wet, and Dry anomalies are only in the first month of the numerical experiments.

3. Results

3.1. Persistence and Reemergence of Precipitation and Air Temperature Anomaly Signals in ST in Observations

ST anomalies caused by air temperature can persist for longer time than those caused by precipitation in shallow soil (Figures 1a and 1b). The persistence duration of shallow ST anomalies caused by air temperature during April–September is about 1 month, while the duration is about 2 months or more in the remaining months. Shallow ST anomalies caused by precipitation from March to October generally persist for about 1 month, and there is no significant ST anomaly persistence at most sites in other months. It can be seen that the persistence of shallow ST anomalies has significant seasonal changes. Moreover, positive air temperature and precipitation anomalies lead to positive and negative shallow ST anomalies, respectively, in the first several months after ST anomalies occur (Figures 1a and 1b).

The reemergence of ST anomalies caused by air temperature is more significant than that caused by precipitation (Figures 1a and 1b). The ST anomaly signals caused by air temperature anomalies at almost all sites have significant reemergence in the first few months of the second year, which may be related to the low temperature in winter. Moreover, the reemergent ST anomalies from positive atmospheric anomalies may be positive or negative (Figures 1a and 1b). The reemergence of ST anomalies may be related to the propagation of ST anomalies at different soil depths, which means that there may be two processes, one is upward propagation of antecedent downward propagated ST anomaly signals after a period of time, and the other may be the process related to the low temperature in winter (Figure 1c; Matsumura & Yamazaki, 2012; Schaefer et al., 2007).

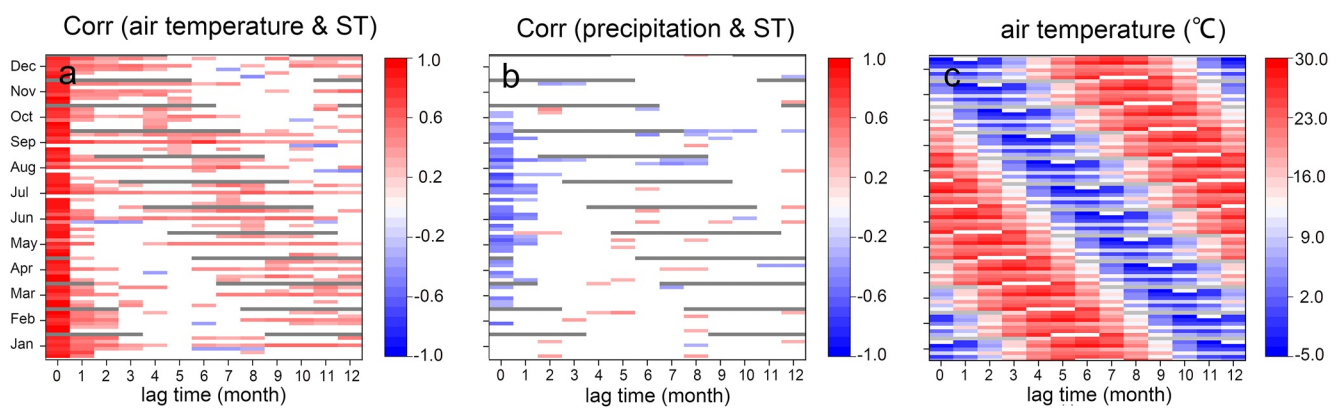

Figure 1. The lag correlation coefficients between air temperature (a) or precipitation (b) and subsequent soil temperature (ST) at the depth of 0.05 m at seven sites in 12 months. (c) is multi-year average air temperature for 12 months with different lag times at seven sites.

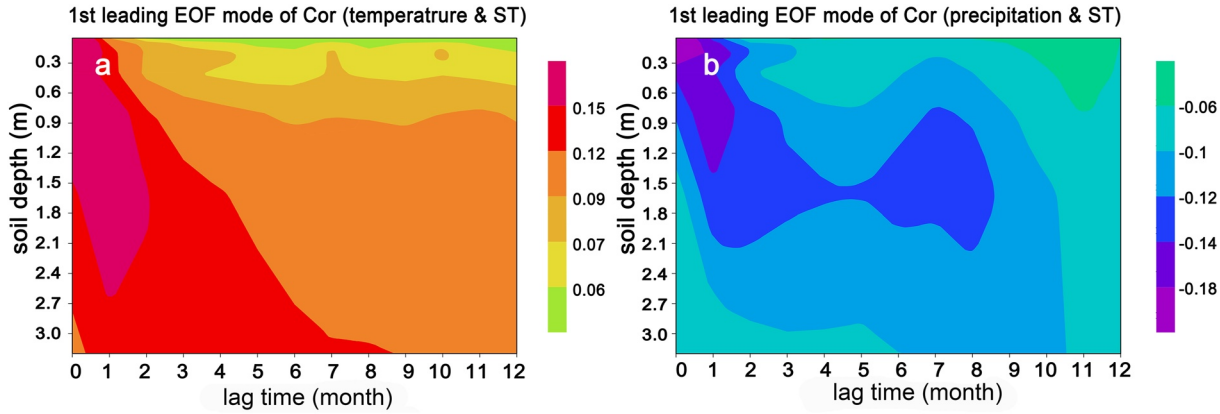

Figure 2. The first leading empirical orthogonal function (EOF) mode (explaining 83.9% or 40.9% variance of total variance) of correlation coefficients between antecedent air temperature or precipitation and soil temperature (ST) at different soil depths with different lag times, and the samples in EOF analysis consist of the correlation coefficients at seven sites in 12 months. (a) is for the correlations between air temperature and ST, (b) is for the correlations between precipitation and ST.

Figure 2 shows the propagation of atmospheric anomaly signals in ST at different soil depths. The first leading EOF modes of the correlation coefficients between air temperature/precipitation and ST (Figures 2a and 2b) show that the anomalies of air temperature and precipitation can persist for about three and 2 months in shallow soil layers, respectively. Air temperature and precipitation signals propagate deep in the soil over time, and air temperature anomaly signals reach about 1.6 and 3.2 m after one and 2 months, respectively. The downward-propagation and attenuation of air temperature signals become less apparent after 3 months. Precipitation signals reach about 1.4 m after 1 month, and the signals stay between 0.9 and 2 m of soil between the lag of three and 10 months. Moreover, the atmospheric signals may return to the shallow soil, especially for precipitation. Unlike in Figure 1a, there are no apparent upward propagated signals in Figure 2a, because anomaly signals propagate upward at almost all lag times, which suppresses the appearance of upward propagated signals in EOF modes.

As shown in Figure 2, the common characteristics of signal propagation are derived from the data at seven sites in 12 months, and the signal-propagation characteristics may be very different at seven sites in 12 months, especially for precipitation signals. Figure 3 shows the variances explained by the first leading EOF modes in Figure 2 for the correlation coefficients between air temperature/precipitation and subsequent ST at seven soil depths and 13 lag times, and the regression coefficients of the correlation coefficients on the first EOF modes in Figure 2. The explained variances and regression coefficients show similar variations at different sites in 12 months. The propagation of ST anomalies caused by precipitation in warm season is closer to the first leading

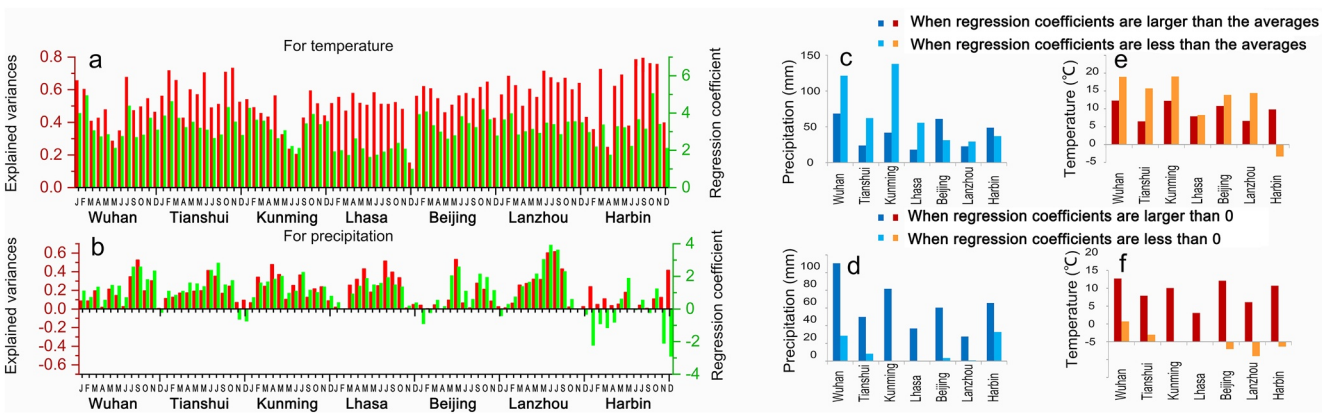

Figure 3. The variances explained (red) by the first leading empirical orthogonal function (EOF) modes in Figure 2 for the correlation coefficients between air temperature (a) or precipitation (b) and subsequent soil temperature (ST), and the regression coefficients (green) of the correlation coefficients on the first EOF modes in Figure 2. (c and e) show the precipitation and air temperature averaged over the months in which regression coefficient is larger or less than regression coefficient averaged over all 12 months at a certain site, respectively. (d and f) show the precipitation and air temperature averaged over the months in which regression coefficient is larger or less than 0 at a certain site, respectively.

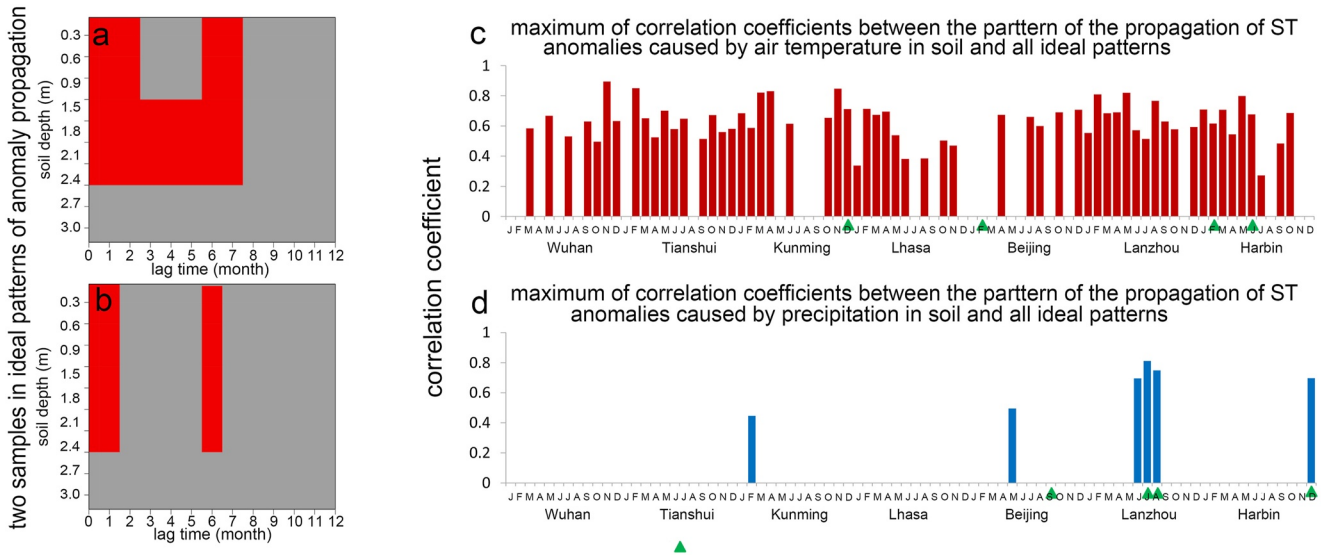

Figure 4. (a and b) are two samples of ideal patterns for the propagation of soil temperature (ST) anomaly signals which may lead to ST anomaly reemergence, and the red and gray are the regions with and without significant anomaly signals, respectively. (c and d) show the maximum of correlation coefficients between the pattern of the propagation of ST anomalies in soil caused by air temperature/precipitation and all ideal patterns at seven sites in 12 months. The selected cases are marked with green triangles.

EOF mode in Figure 2b than in cold season, except at Harbin site (Figure 3b). At Beijing, Lanzhou and Harbin sites, the time-dependent changes in ST anomalies at different soil depths caused by winter precipitation have opposite patterns to the first leading EOF mode in Figure 2b, especially at Harbin site (Figure 3b), which may be related to the air temperature close to or below 0°C in winter (Figure 3f). The changes of ST anomalies over time caused by air temperature anomalies in all months are very consistent with the first leading EOF mode in Figure 2a, especially in cold season (Figures 3a and 3e). Therefore atmospheric conditions may play an important role in the response of ST to atmospheric anomalies.

In addition to the persistence in shallow soil, the reemergence of ST anomalies also makes it possible for antecedent anomalies to affect subsequent atmosphere. The reemergence of ST anomalies generally can be caused by two processes. One includes the downward propagation, storage and upward propagation of ST anomaly signals in soil caused by atmospheric anomalies. The other is related to the reappearance of ST anomaly signals previously stored in soil freezing after soil thawing. To find the months in which ST anomalies may reemerge after a period of time at the seven sites, a series of ideal patterns for the propagation of ST anomaly signals which may lead to ST anomaly reemergence are established. Figures 4a and 4b show two samples of the ideal patterns. Some cases related to ST anomaly reemergence are determined by the maximum of correlation coefficients between the ideal patterns and the patterns of ST anomaly propagation at different soil depths with 13 lag times caused by atmospheric anomalies. Moreover, in the above selected cases, the cases without significant previous downward and subsequent reappearance of ST anomaly signals are removed. Figures 4c and 4d show the cases that may result in the reemergence of ST anomalies. It' is obvious that the reemergence of air temperature-induced ST anomalies occur in more months than those caused by precipitation, which may be because ST is more sensitive to air temperature than precipitation. It may be different if the response of soil moisture to atmospheric anomalies is studied.

To analyze the reemergence of ST anomaly signals and the corresponding atmospheric conditions, eight cases are selected from the 12 months at seven sites in Figures 4c and 4d. Two cases without ST anomaly reemergence are also selected to compare and analyze the differences in atmospheric conditions under which ST anomaly reemergence occurs or not. For the signal propagation caused by precipitation (Figure 4d), the precipitation anomalies in the four selected cases are at Beijing site in September, at Lanzhou site in July, at Lanzhou site in August and at Harbin site in December. There is not the reappearance of ST anomaly signals at Beijing site in September. For the signal propagation caused by air temperature, the air temperature anomalies of the other four selected cases are at Kunming site in December, at Beijing site in February, at Harbin site in February and at Harbin site in June, respectively. There is not the reappearance of ST anomaly signals at Beijing site in February.

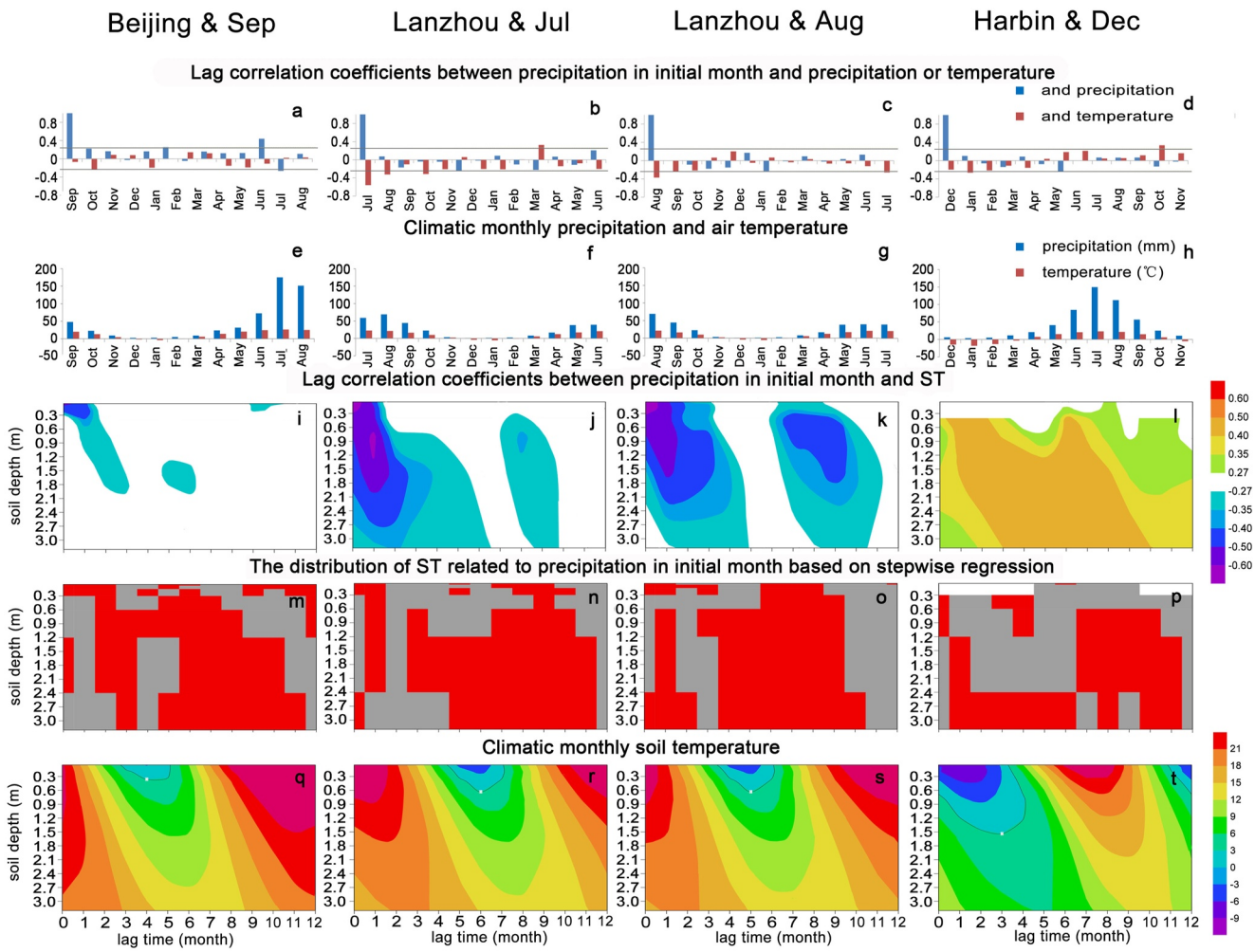

Figure 5. The case analysis of the relationships between the precipitation in initial month and soil temperature (ST), which includes the cases at Beijing site in September (a, e, i, m, q), at Lanzhou site in July (b, f, j, n, r), at Lanzhou site in August (c, g, k, o, s) and at Harbin site in December (d, h, l, p, t). (a, b, c, and d) are lag correlation coefficients between the precipitation in initial month and subsequent precipitation/temperature; (e, f, g, and h) are climatic monthly precipitation and air temperature; (i, j, k, and l) are the lag correlation coefficients between the precipitation in initial month and subsequent ST; (m, n, o, and p) are the distributions of ST related to the precipitation in initial month based on stepwise regression; (q, r, s, and t) are climatic monthly ST. The black lines in (q, r, s, and t) represent the 0°C contour. The shaded areas in (i, j, k, l, m, n, o, and p) represent 95% confidence intervals. The gray lines represent 95% confidence intervals in (a–d). The red and gray are the regions with and without significant anomaly signals, respectively in (m–p).

Figures 5 and 6 show the propagation of air temperature and precipitation anomaly signals in ST in the eight selected cases in Figure 4, respectively. Except at Harbin site in December, the increases of precipitation at Beijing site in September, at Lanzhou site in July and August lower the concurrent and subsequent ST. Precipitation signals in September propagate downward in the first 3 months, and disappear after 7 months at Beijing site (Figure 5i). There are significant signals at the soil depths between 1.2 and 1.8 m at the lag of five and 6 months, and the signals may be attributed to the previously stored ST anomaly signals, because the lag correlation coefficients between PIM and the precipitation or air temperature at the lag of five and 6 months are not significant (Figure 2a), suggesting that the weak signals may not come from the instantaneous precipitation or air temperature. Moreover, the results of stepwise regression analysis show that PIM is a necessary part of the signals leading to the anomalous ST signals at the lag of five and 6 months (Figure 5m). When atmospheric anomalies disappear, ST anomalies in shallow soil also disappear (Figure 5i).

Compared to Figure 5i, there are stronger signal storage of PIM in ST shown by Figures 5j, 5k, and 5l. Similar to the case in September at Beijing site, ST anomaly signals reappearance in the cases at Lanzhou site in July, at Lanzhou site in August and at Harbin site in December because of the reasons shown in Figures 5b–5d and 5n–5p similar to the ones in Figures 5a and 5m. But there is still a confusing feature, that is, there are

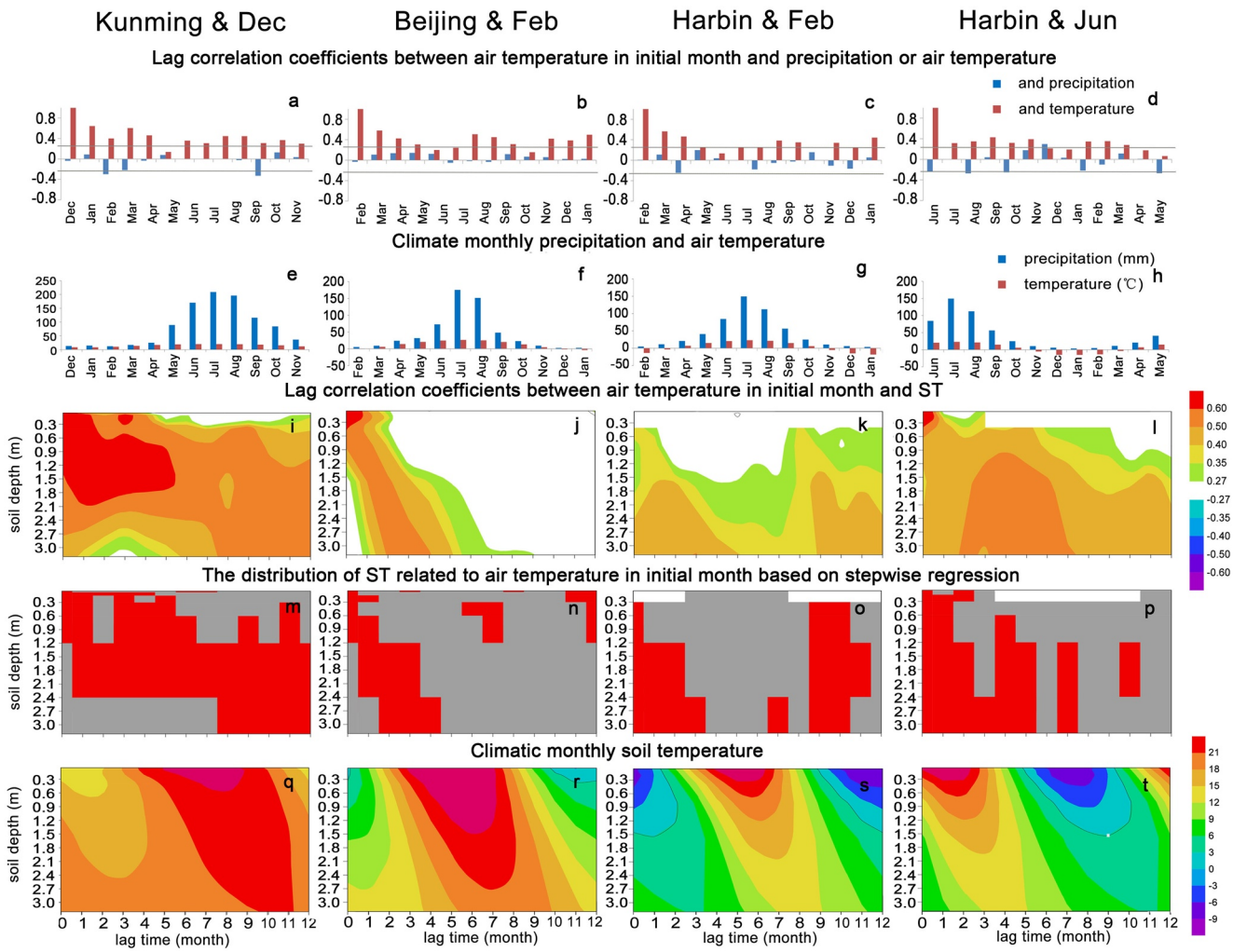

Figure 6. Same as Figure 5, but for the relationships between the air temperature in initial month and soil temperature (ST).

regions with low correlation between the time of ST anomaly signal reappearance and the first few months in Figures 5i–5k, which might be explained by freeze-thaw process (Matsumura & Yamazaki, 2012; Schaefer et al., 2007). In Figure 5l, the correlation between PIM and ST is positive, which may be related to low ST. When ST is below freezing (Figures 5h and 5t), more precipitation leads to thicker and more ice above and in the soil, and the ice blocks the infiltration of cold rainwater and insulates the effect of cold air temperature on the ST under frozen soil, resulting in higher ST. Moreover, Figures 5j and 5k show that atmospheric anomaly signals cannot persist in ST in shallow soil once atmospheric anomalies in July at Lanzhou site disappear, but the anomalies can persist for about 3 months after atmospheric anomalies disappear in August at Lanzhou site.

As shown in Figures 5q, 5r, and 5s, the downward propagation and reemergence of PIM signals in ST corresponds to the periods before and after soil freezing, respectively. During freezing season, ST anomaly signals are stored in frozen soil or isolated from the atmosphere by frozen soil. When soil thaws, the precipitation anomaly signals in initial month reappear in the form of ST anomalies. From the perspective of freeze-thaw mechanism, more precipitation in warm season results in thicker freezing soil in cold season, requiring more energy to thaw in next warm season, and then resulting in colder soil in the next warm season (Matsumura & Yamazaki, 2012; Schaefer et al., 2007). But the precipitation signals in December in Harbin shows a different feature. The downward and upward propagation of PIM signals occurs during cold and warm periods, respectively (Figures 5h and 5t). More precipitation in the initial month results in thicker frozen soil and higher coverage of frozen soil, which prevents the infiltration of cold rainwater and insulates the effect of air temperature on the ST under frozen soil, resulting

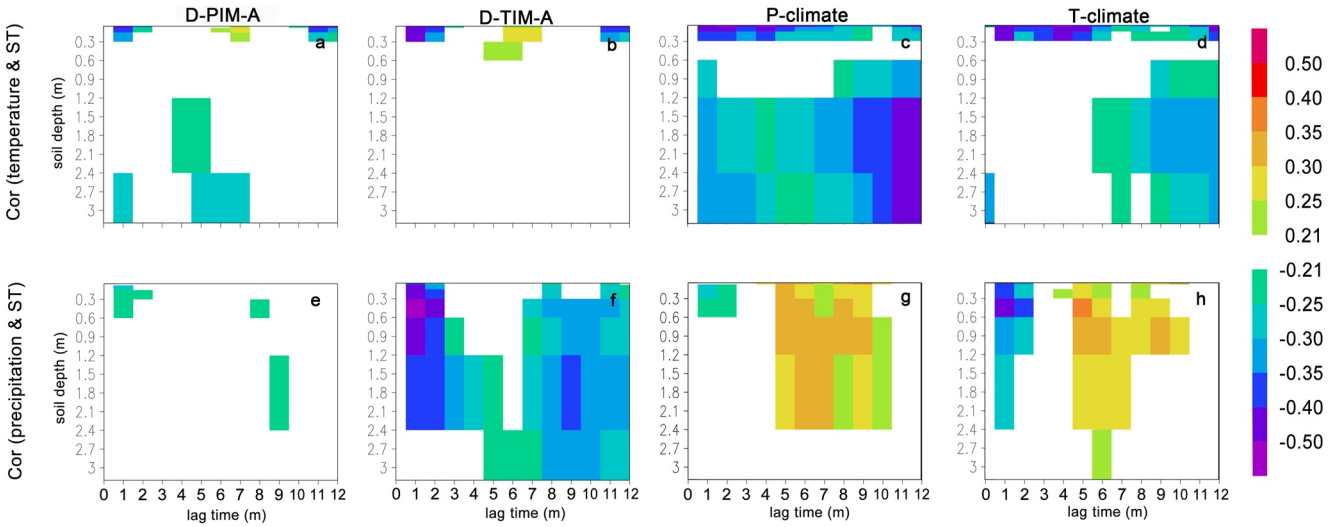

Figure 7. The correlation coefficients between D-PIM-A/D-TIM-A/P-climate/T-climate and C-TIM-ST/C-PIM-ST. (a) is for D-PIM-A and C-TIM-ST, (b) is for D-TIM-A and C-TIM-ST, (c) is for P-climate and C-TIM-ST, (d) is for T-climate and C-TIM-ST, (e) is for D-PIM-A and C-PIM-ST, (f) is for D-TIM-A and C-PIM-ST, (g) is for P-climate and C-PIM-ST, (h) is for T-climate and C-PIM-ST. The shaded areas represent 95% confidence intervals.

in higher ST. Moreover, when cold season is longer and air atmospheric temperature is lower, thicker frozen soil takes longer time to thaw, delaying the reemergence of anomalous signals.

The ice from precipitation acts as a water and thermal insulation between soil and atmosphere, and it prevents subsequent cold rainwater from infiltrating into the soil, thus more precipitation results in higher ST. When the atmospheric temperature is lower or low air temperature persists for longer time, thicker frozen soil takes longer time to thaw, delaying the reappearance of anomalous signals, and the reemergence of ST anomalies may occur in the next warm season.

The ST anomalies caused by air temperature anomalies can persist from two to 4 months in shallow soil for the four cases shown in Figure 6, and the anomalies can persist longer time in cold season than in warm season, which is consistent with the analysis shown in Figure 1. Figures 6i–6l show that there are significant positive correlations between TIM and the subsequent ST, indicating that higher air temperature leads to higher ST. There are reemergence of anomaly signals in Figures 6i, 6k, and 6l, except in Figure 6j. Unlike PIM (Figures 5a–5d), the lag correlation between TIM and subsequent temperature or precipitation is significantly larger (Figures 6a–6d). Is the high autocorrelation of air temperature the cause of the reappearance of anomaly signals? However, in the period when there are no reemergent anomaly signals, there are also significant correlations between TIM and air temperature; thus the autocorrelation of air temperature may not be the main reason. Moreover, based on stepwise regression analysis, the signal of TIM is a necessary part of the antecedent signals leading to the later reemergent anomaly signals in Figures 6m, 6o, and 6p. Therefore the upward propagation of previously downward-propagating ST anomalies may be the cause of the reemergence of ST anomalies in Figures 6i, 6k, and 6l.

Although some data are missing (Figures 6k and 6l), referring to the conclusions of the regression analysis, the signals may propagate upward during the transition from warm-wet to cold-dry (Figures 6m, 6o, 6p, 6q, 6s, and 6t). For the TIM at Beijing site in February, the signals propagate downward over time, but not propagate upward to shallow soil (Figure 6j). In Figure 6b, there are significant autocorrelation of air temperature, and the distributions of air temperature and precipitation are similar to Figures 6e and 6g; therefore whether the signals can propagate upward also be affected by other factors, such as the interactions of the variables in soil.

The reemergence of PIM signals in ST occurs when air temperature and precipitation are low (Figures 5e–5g), but not for the PIM signals at Harbin site in December. The upward propagation of the signals caused by air temperature anomalies occurs during the transition from warm-wet to cold-dry (Figures 6e, 6g, and 6h). Therefore, climatic condition may be an important factor in the upward propagation of the signals stored in ST, which also can be expressed as the reemergence of the signals. Moreover, the strength of atmospheric signals in initial month may also be important in the signal propagation.

The effects of the degree of air temperature and precipitation anomalies in initial month (D-TIM-A, D-PIM-A) on the signal propagation are shown in Figures 7a, 7b, 7e, and 7f, and the effect of climatic conditions are also shown in Figures 7c, 7d, 7g, and 7h. Except for the relationships between P-climate/T-climate and the correlations between PIM and ST (C-PIM-ST; Figures 7g and 7h), there are obvious negative correlations in other relationships (Figures 7a–7f).

The correlations between TIM and ST (C-TIM-ST) become weaker with the increase of the degree of air temperature/precipitation anomalies in initial month, P-climate and T-climate (Figures 7a–7d). As P-climate and T-climate rise, the intensity of atmospheric interference with the correlations between TIM and ST increase, and it leads to the negative correlation between P-climate or T-climate and the correlations between TIM and ST. However, how the change in the degree of TIM or PIM anomalies affects the correlations between TIM and ST is puzzling and needs further studied. The effects of the degree of PIM and TIM anomalies on the correlations between TIM and ST are mainly in shallow soil in the 2 months following the month of TIM (Figures 7a and 7b), and the significant correlations at the lag of six and twelve months may only be related to the autocorrelation of air temperature. The effect of P-climate on the correlations between TIM and ST in shallow soil may be attributed to the noise caused by instantaneous precipitation, and the effect in deep soil may be related to the cooling effect of rainwater infiltration. The effect of T-climate on the correlations between TIM and ST in shallow soil may be caused by instantaneous air temperature, and the effect in deep soil may be attributable to the high correlation between precipitation and air temperature.

With the increase of the degree of air temperature and precipitation anomalies in initial months, the negative and positive correlations between PIM and ST strengthens and weakens, respectively (Figures 7e–7h). The effect of the degree of PIM anomalies on the correlations between PIM and ST is mainly at the lag of one and 2 months (Figure 7e), and the significant correlations at the lag of eight and 9 months be related to the freeze-thaw processes. The characteristics of the effect of the degree of TIM anomalies on the correlations between PIM and ST is similar to the characteristics of the correlations between PIM and ST at different soil depths and different lag times (Figure 7f), which may be related to the differences of the physical processes under different air temperature conditions (Figures 5f–5h and 5j–5l). Differences of climatic air temperature also lead to the negative and positive correlations between T-climate/R-climate and the correlations between PIM and ST at lags of 1–2 months and 5–10 months, respectively (Figures 5f–5h, 5j–5l, and 7g–7h).

The analysis of the observations shows the characteristic of anomaly signals propagation in ST caused by atmospheric anomalies and the effect of the degree of atmospheric anomalies in initial months or climatic conditions on signal propagation. Can the characteristics be reproduced in land surface simulations? How long can ST anomalies caused by atmospheric anomalies persist in shallow soil? And is there also the reemergence of ST anomaly signals? Moreover, what are the physical processes related to the propagation of air temperature and precipitation signals in ST? How much influence do climatic conditions, the degree of TIM and PIM anomalies have on the signal propagation in ST? Can the conclusions drawn by statistical analysis be obtained by numerical simulation?

3.2. Persistence and Reemergence of Precipitation and Air Temperature Anomaly Signals in ST in the Simulations by CLM4.5

Based on the simulations using CLM4.5, ST anomaly signals caused by air temperature or precipitation in the initial month can persist until at least next month, which is manifested as the anomalies of land surface variables in shallow soil (Figure 8). It is very obvious that climatic conditions, especially air temperature, have important influence on the subsequent variations of land surface variables caused by the anomalies of TIM or PIM. In the real atmosphere, the changes of air temperature and precipitation are often accompanied by the changes of atmospheric humidity. Sensitivity simulations show that the anomalies of land surface variables are significantly larger when atmospheric humidity changes with precipitation or air temperature in the initial months than when atmospheric humidity does not change with air temperature or precipitation in the initial month (Figure 8). The anomalies of land surface variables caused by the TIM are larger than the ones caused by PIM, and the anomalies are relatively weak in the T1R05, T1R1, and T1R2 conditions. The anomalies caused by the dry/cold and wet/warm anomalies are in opposite phases. The most affected land surface variables are sensible heat flux (SH), ground evaporation (GEV), emitted near-infrared radiation (EIR), (heat flux into soil) GR, ground temperature (Tg), absorbed solar radiation (SABS), soil water at 0.7 cm soil depth (SW0.7 cm), soil water at 2.9 cm

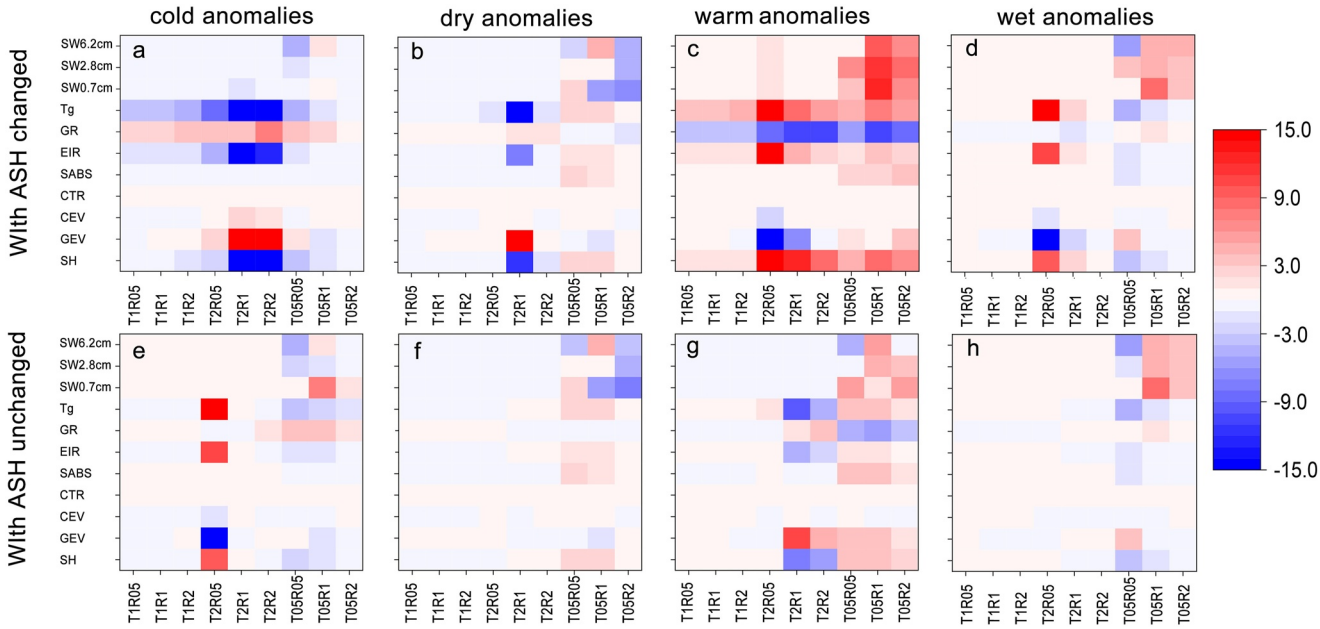

Figure 8. The anomalies of land surface variables in the second month of the simulations caused by the anomalies of air temperature and precipitation in the first month of the simulations under nine atmospheric conditions with two configurations of atmospheric specific humidity in CLM4.5. (a and e) are for low temperature in the first month, (b and f) are for low precipitation in the first month, (c and g) are for high temperature in the first month, (d and h) are for high precipitation in the first month. The meaning of the abbreviations for land surface variables refers to the text.

(SW2.9 cm) and soil water at 6.2 cm (SW6.2 cm). Canopy evaporation (CEV) and transpiration (CTR) are less affected (Figure 8).

Cold anomalies can lead to larger anomalies of land surface variables in the T2R1 and T2R2 conditions when atmospheric specific humidity (ASH) changes accordingly with the TIM and PIM anomalies (Figure 8a), but larger anomalies appear in the T2R05 condition when ASH does not changes (Figure 8e). For warm anomalies, the corresponding anomalies are larger with ASH changing than without ASH changing, especially in the T2R05 condition (Figures 8c and 8g). Dry anomalies can lead to larger anomalies in the T05R05, T05R1, and T05R2 conditions (Figures 8b and 8f). In the T2R1 condition, the anomalies caused by dry anomalies are significantly stronger when ASH changes (Figures 8b and 8f). For wet anomalies, the resulting anomalies are obvious in the T05R05, T05R1, and T05R2 conditions, and the resulting anomalies in the T2R05 and T2R1 conditions are obviously larger when atmospheric anomalies are accompanied with ASH changing (Figures 8d and 8h).

Warm/Cold anomalies of TIM lead to positive/negative Tg anomalies, which are consistent with observations (Figures 6i–6l). Wet/Dry anomalies of PIM lead to negative/positive Tg anomalies in the T05R05, T05R1, and T05R2 conditions, with good agreement with the observations (Figures 5i–5k). In the T2R05, T2R1 conditions, the positive/negative Tg anomalies are caused by wet/dry anomalies, consistent with the observations (Figure 5l). Climatic air temperature in the T2R1/T2R2 is higher than the one in the T05R05/T05R1/T02R2, which corresponds to the positive and negative anomalies of Tg caused by wet anomalies, respectively. However, higher climatic air temperature in Figures 5i–5k and lower one in Figure 5l correspond to negative and positive correlations between PIM and ST, respectively, which is different from the conclusion shown in Figure 8.

Figure 9 shows the variations of the anomalies of land surface variables in the second month caused by TIM and PIM with T-climate, P-climate, the degree of TIM and PIM anomalies. The responses of the anomalies in land surface variables caused by atmospheric anomalies in the first simulation months to the change of T-climate and P-climate are very complex, which is obviously different from the single negative correlations shown in the first several months in Figure 7. A positive correlation between Tg anomalies and T-climate is noted when P-climate is low (Figure 9a), which is inconsistent with the observation analysis (Figures 7d and 7h). A negative correlation between Tg anomalies and R-climate is found when T-climate is low (Figure 9a), which is consistent with the observation analysis (Figures 7c and 7g). Moreover, Tg anomalies decrease when the degree of TIM anomalies increases, and it is consistent with the observation analysis (Figures 7b and 7f). However, Tg anomalies caused by

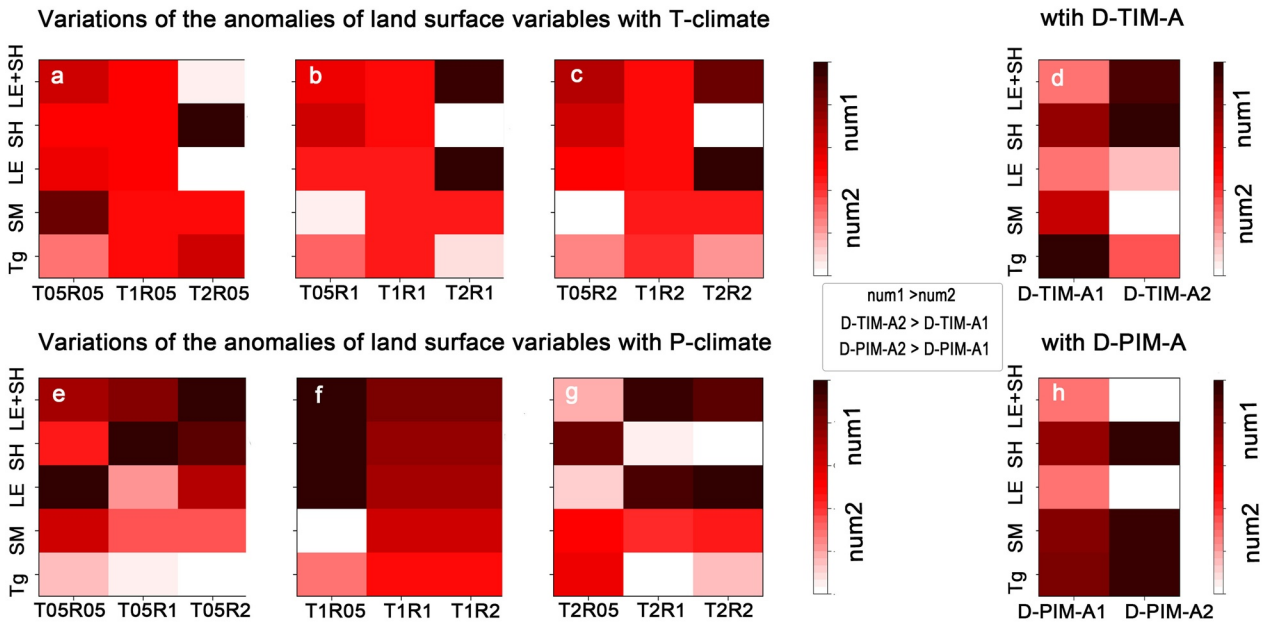

Figure 9. The responses of the anomalies of land surface variables in the second month of the simulations caused by the anomalies of temperature and precipitation in the first month under different atmospheric conditions to the degree of precipitation/temperature anomalies in the first month (D-PIM-A/D-TIM-A) and atmospheric conditions (P-climate/T-climate). (a–) are the variations of the anomalies of land surface variables with T-climate; (e–g) are the ones with P-climate; (d and h) the variations of the anomalies of land surface variables with D-TIM-A and D-PIM-A, respectively.

atmospheric anomalies in the first simulation months increase with the increase of the degree of PIM anomalies, different from the observation analysis (Figures 7a and 7e).

How long can ST anomalies caused by atmospheric persist in shallow soil? Is there ST anomaly reemergence in the simulations using CLM4.5? Figure 10 shows that ST anomalies can persist longer in shallow soil in the T05R2, T05R1, T05R05 conditions than in the other conditions. The ST anomalies caused by air temperature

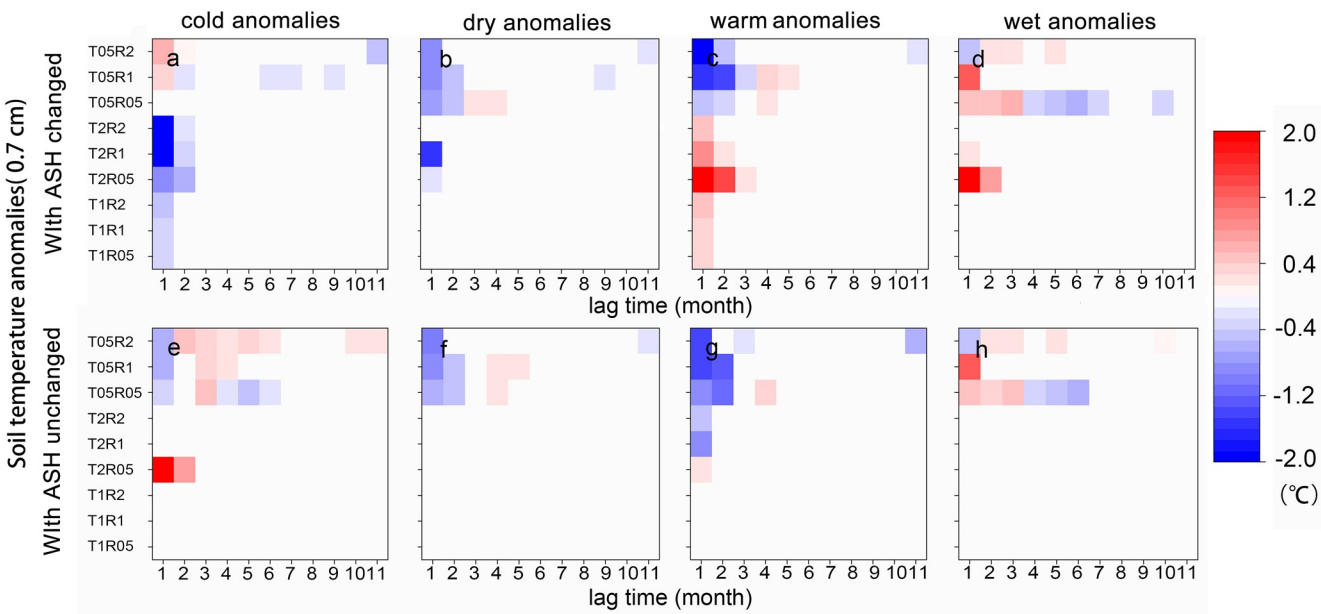

Figure 10. The persistence and reemergence of the soil temperature (ST) anomalies at a depth of 0.7 cm caused by the anomalies of temperature and precipitation in nine atmospheric conditions with two configurations of atmospheric specific humidity in CLM4.5. (a and e) are for low temperature in initial month, (b and f) are for low precipitation in initial month, (c and g) are for high temperature in initial month, (d and h) are for high precipitation in initial month.

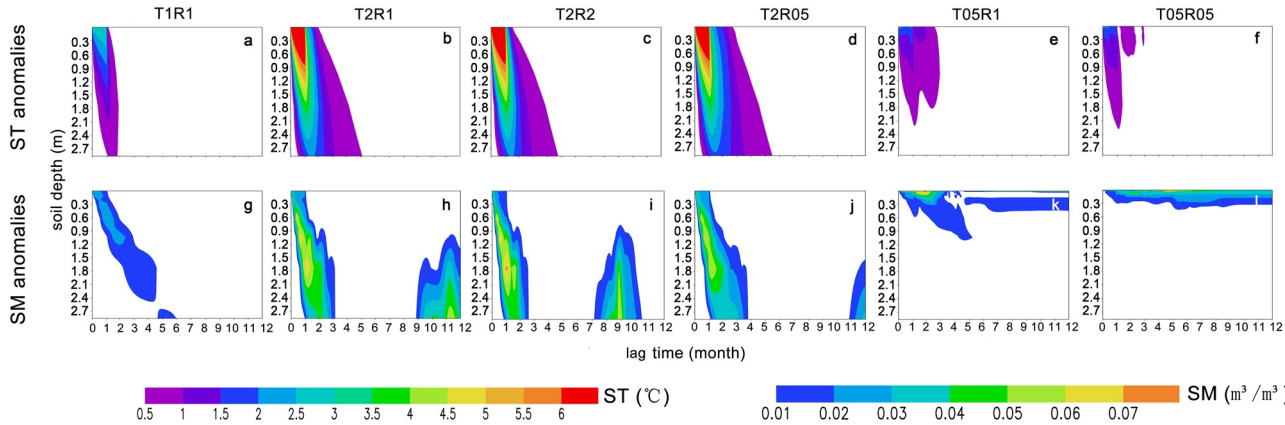

Figure 11. The variations of the simulated soil temperature (ST) and soil moisture anomalies caused by temperature and precipitation anomalies in the first month of the simulations under different atmospheric condition. (a, b, c, d, e, and f) are the anomalies of ST; (g, h, i, j, k, and l) are the anomalies of soil moisture (SM).

anomalies can persist longer than those caused by precipitation anomalies, which is consistent with the observations (Figure 1). When ASH does not change with atmospheric anomalies, the ST anomalies caused by precipitation and air temperature anomalies can persist for zero and about one month, respectively, except in the T05R2, T05R1, and T05R05 conditions. The reemergence of ST anomalies only can be found in the T05R1, T05R2, and T05R05 conditions, and the characteristics of persistence and reemergence of ST anomalies are quite different in the T05R05, T05R1, and T05R2 conditions. In T05R05, T05R1, and T05R2 conditions, soil freezing occurs.

Based on observations, the reemergence of ST anomaly signals in shallow soil often occurs, especially those caused by air temperature (Figures 1 and 6). Figure 10 also shows the reemergence of ST anomalies simulated by CLM4.5. The persistence and reemergence of ST anomalies in shallow soil are the manifestation of the signal propagation caused by atmospheric anomalies in soil, which are related to the storage and propagation of anomaly signals in the whole soil column, so what are the characteristics of the storage and propagation of atmospheric anomalies in soil simulated by CLM4.5?

Figure 11 shows the mean absolute values of simulated ST and soil moisture anomalies caused by the TIM and PIM anomalies. In the first month of the simulations, which is the initial month, land surface processes are driven by anomalous atmosphere. Significant downward propagating signals are found in ST and soil moisture (Figure 11). In the T1R1 condition, the ST anomalies caused by atmospheric anomalies are not significant after atmospheric anomalies disappear, in other words, atmospheric anomaly signals cannot persist and be stored in ST under the T1R1 condition (Figure 11a). Soil moisture can store atmospheric anomalies in deep but not shallow soil due to the downward propagation of soil moisture anomaly signals caused by atmospheric anomalies over time (Figure 11g). Compared to the T1R1 condition, ST anomalies can persist longer in the whole soil column in the T2R1, T2R2, T2R05, T05R1, and T05R05 conditions. Unlike in the T2R1, T2R2, and T2R05, the ST and soil moisture anomaly signals are mainly concentrated in the shallow and middle layers of the soil (Figures 11e, 11f, 11k, and 11l) because soil freezing caused by low-temperature block the downward propagation of anomaly signals, and the anomaly signals are stored in the form of soil freezing in the T05R1 and T05R05 conditions. In the T2R1, T2R2, and T2R05 conditions, the signals of soil moisture anomalies propagate upward after several months because of the anomalies of water table due to the suppression of evapotranspiration by high atmospheric humidity corresponding to high air temperature and ST anomalies can persist longer in shallow soil when instantaneous precipitation decreases (Figures 11b–11d) due to the reduction of interference signals from instantaneous precipitation, which is consistent with the results based on the observations (Figure 7c).

Except for the T1R1 condition, the ST anomalies caused by atmospheric anomalies can persist for at least 1 month. Soil moisture anomalies weaken rapidly after atmospheric anomalies disappear except in the cases with soil freezing. In the T2R1, T2R2, and T2R05 conditions, soil moisture anomaly signals do not propagate upward to the land surface, thus not causing the reemergence of ST anomalies in shallow soil. As shown in Figures 11e, 11f, 11k, and 11l, the persistence and reemergence of ST anomaly in shallow soil are closely related to soil freezing in the T05R1 and T05R05 conditions. However, the reemergence of ST anomalies cannot be found in the other atmospheric conditions in the simulations using CLM4.5 (Figure 11), which may be attributed to the unchanged

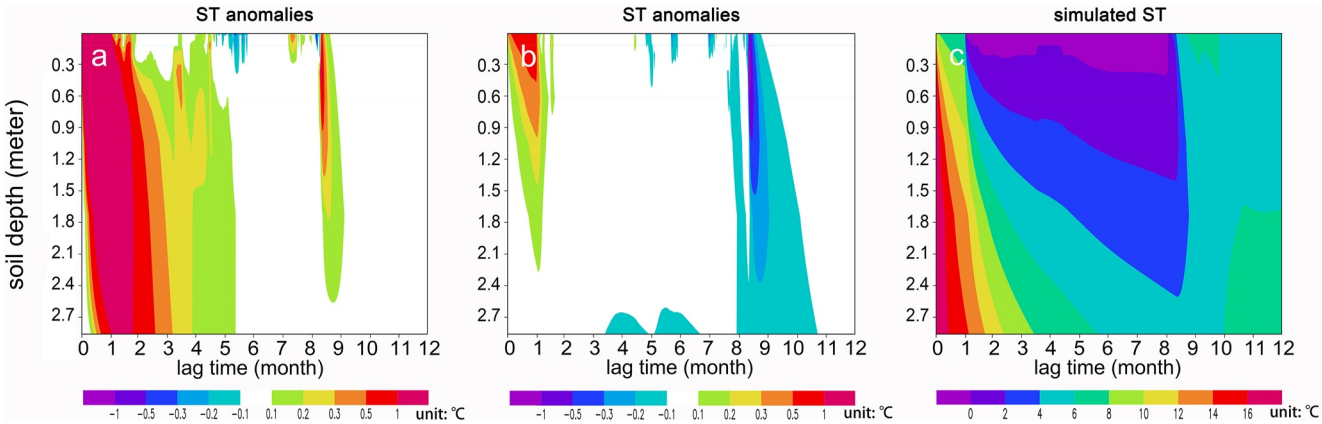

Figure 12. The time-varying variations of the simulated soil temperature (ST) anomalies at different soil depths caused by air temperature and precipitation anomalies in the first month under the FT condition. (a and b) correspond to the positive anomalies of air temperature and precipitation, respectively; (c) is the simulated ST in control experiment.

atmospheric conditions except in the initial month. However, based on the simulations in two sets of experiments with atmospheric conditions similar to the situations shown in Figures 6e, 6g, and 6h, the reemergence of ST anomalies does not occur, except for those associated with the freeze-thaw processes (Figure S1 in Supporting Information S1). Moreover, based on the information presented in Figures 1, 5, 6, and 11, the atmospheric conditions that lead to soil freezing and thawing may be important for the reproduction of ST anomaly reemergence in shallow soil in the numerical simulations.

Under FT atmospheric condition, air temperature is below 0°C during the first to eighth months after the initial month, which results in soil freezing at the corresponding time (Figure 12c). Regardless of ST anomalies caused by air temperature or precipitation, the reemergence of ST anomalies occurs when soil thaws (Figures 12a and 12b). The increase in air temperature leads to warmer ST, which causes thinner frozen soil. During warm season, the thawing of thinner frozen soil consumes less heat, which further resulting in higher ST (Figure 12a). Because atmospheric condition changes after the initial month, higher ST in deep soil caused by positive air temperature anomalies in the initial month changes the vertical thermal conductivity, and leads to soil thawing from the bottom of frozen soil during cold season, suggesting the upward propagation of ST anomaly signals due to the change of atmospheric conditions (Figure 12a). The increase of precipitation is accompanied by an increase of atmospheric humidity, which suppresses evapotranspiration. The reduction of evapotranspiration helps to retain heat in soil, and further leads to the positive ST anomalies (Figure 12b). During cold season, ST anomaly signals are stored in frozen soil, and are released in the next warm season. The infiltration of rainwater increases the specific heat capacity of the soil, which suppresses the increase of ST during warm season resulting in the negative ST anomalies (Figure 12b). It is obvious from the above that freeze-thaw process is one of the important processes that leads to the reemergence of ST anomalies in shallow soil, which has been proved in both observations and simulations. Moreover, it is found that the downward-propagating ST anomaly signals may propagate to shallow soil after a period of time when atmospheric conditions change (Figures 5l, 6i, 6k, 6l, and 12a).

4. Conclusions and Discussion

Antecedent atmospheric anomalies can affect subsequent atmosphere by land surface processes, and the processes are related to the persistence of land surface variable anomalies in shallow soil and the reemergence of land surface variable anomalies in shallow soil caused by antecedent atmospheric anomalies. The ST anomalies caused by air temperature and precipitation can persist from zero to several months in shallow soil, and those caused by air temperature anomalies can persist longer than ones caused by precipitation anomalies. The persistence duration of ST anomalies caused by air temperature during April–September is about 1 month, while the duration is about 2 months or more in the remaining months. The ST anomalies caused by precipitation from March to October usually only persist for about 1 month. Moreover, our analysis suggests that the ST anomalies caused by initial atmospheric anomalies can reappear in shallow soil by two ways. One is that the downward-propagating ST anomalies propagate upward after a period of time, and the other is that the ST anomalies are stored in other

form and then cause later ST anomalies. Soil freezing is an important form of the storage of ST anomaly signals in soil. The reemergence of ST anomalies from air temperature is a more common phenomenon than the one from precipitation.

Observation analysis shows that the signals of air temperature and precipitation anomalies stored in ST propagate downward with time. Based on the stepwise regression analysis on the relationships between the ST at a certain soil depth in a certain month and air temperature/precipitation from 0 to 12 months in advance, we can determine whether air temperature/precipitation in the initial month is a necessary part of the signals that constitutes the subsequent ST anomaly signals at the certain soil depth in the certain month. The changes of ST depend on the changes of antecedent and concurrent atmospheric anomalies, and the main variables affecting ST include air temperature and precipitation; therefore, ST anomaly signals are derived from antecedent and concurrent air temperature/precipitation signals. The correlations between precipitation in the initial month and subsequent air temperature/precipitation show ST anomaly signals, which are closely related to the precipitation anomalies in the initial month, are not from the instantaneous air temperature/precipitation (Figures 5 and 6). Furthermore, the climate means of air temperature, precipitation, and ST show freeze-thaw process may be the key in the reemergence of ST anomalies in shallow soil (Figures 1c, 5i–5k, and 12). The ST anomaly signals caused by atmospheric anomalies are stored in frozen soil, and then are released when soil thaws. Moreover, the change of atmospheric conditions may cause the upward propagation of anomaly signals previously stored in middle and deep soil layers by changing vertical thermal and hydraulic conductivities (Figures 5l, 6i, 6k, 6l, and 11a), manifesting as the reemergence of anomaly signals. Frozen soil blocks the exchange of water and heat between soil and atmosphere, which is favorable to the storage of antecedent atmospheric anomaly signals in soil. Kumar et al. (2019) confirmed that atmospheric condition anomalies can cause the changes of soil hydraulic conductivity, which may further cause "soil moisture reemergence." Previous studies have confirmed that freeze-thaw process plays an important role in the storage and reemergence of ST anomalies (Matsumura & Yamazaki, 2012; Schaefer et al., 2007). But in December at Harbin, positive precipitation anomalies in initial months result in positive ST anomalies, which is different from the other cases in Figure 5. The related process may be that more precipitation in the initial month results in thicker frozen soil and higher coverage of frozen soil, which prevents the infiltration of cold rainwater and insulates the effects of air temperature on the ST under frozen soil during the subsequent cold season, resulting in higher ST. Soil thawing restarts the exchange of water and heat between soil and atmosphere during the next warm season, which means the upward propagation of anomaly signals in soil.

The relationships between antecedent air temperature and ST (Figures 1a and 6) may correspond to two different processes, respectively. Freeze-thaw process may be the main reason for most ST anomaly reemergence shown in Figure 1a. As shown in Figure 6, the results of stepwise regression analysis show air temperature/precipitation in the initial month is essential for the formation of subsequent ST anomaly signals (Figures 6i, 6k, and 6l). Although there are significant correlations between air temperature in the initial month and subsequent air temperature, the significant correlations are distributed not only when anomaly signals propagate upward but also when the signals do not propagate upward (Figure 6); therefore, the signals of ST anomalies propagating upward may not be from instantaneous air temperature. With reference to climate average temperature, precipitation, and ST in 12 months (Figure 6), the upward propagation of anomaly signals cannot be explained by freeze-thaw mechanism in Figure 6, which is different from that shown in Figure 1a. Anomaly signals propagate upward during the transition from warm-wet to cold-dry (Figure 3); therefore, climatic condition may be an important factor in the upward propagation of the signals stored in ST. When the climate shifts from warm-wet to cold-dry, the decrease in air temperature and precipitation leads to the changes of the vertical distributions of hydraulic and thermal conductivities (Figures 6i, 6k, and 6l), which may account for the upward propagation of ST anomalies shown in Figure 6.

In numerical simulations using CLM4.5, the persistence of anomalous signals in shallow soil has similar characteristics to observation analysis. Atmospheric anomaly signals can be stored in frozen soil when ST is below 0°C in numerical simulations (Figures 10k and 10l), similar to the studies of Schaefer et al. (2007). They found the past ST anomalies are stored as the variations in the amount of ice and can reemerge at the surface after frozen soils thaw using a soil heat transfer model by adjusting ground surface heat flux and ST in the initial month.

The reemergence of ST anomalies plays an important role in climate predictions, whether it can be reproduced in numerical simulations is essential. However, there is no reemergence of ST anomalies, except when soil freezing and thawing occur in the numerical simulations shown in this paper using CLM4.5. In addition to the freeze-thaw

process, the variations of vertical distributions of ST and soil moisture caused by atmospheric conditions may be the cause of upward propagation of previously downward-propagating ST anomaly signals caused by atmospheric anomalies (Figure 6). Except for the upward propagation of anomaly signal related to soil freezing shown in Figure 12a, the signal propagation processes shown in Figures 6i, 6k, and 6l cannot be reproduced by CLM4.5. In addition, we cannot be 100% sure that the upward-propagating signals are from atmospheric anomalies in the initial month, although it is an inference based on the observation analysis (Figure 6).

According to the observation analysis, the enhanced PIM/TIM weakens the correlations between TIM/PIM and ST. The increase of T-climate and P-climate inhibits the storage and propagation of atmospheric anomaly signals in ST. However, in the numerical experiments, the responses of ground temperature anomalies to the TIM/PIM anomalies are very complex with different degree of TIM/PIM anomalies under different atmospheric conditions, which is not completely inconsistent with the conclusions obtained from the observations. The possible reasons are the selection of the sites, soil composition, atmospheric conditions used in the numerical experiments, and simulation performance of land surface model, which may require more sites and more land surface models for further verification. Moreover, soil moisture also is an important indicator of soil heat storage, and is a key factor for the response of soil to atmospheric anomalies; therefore, the anomalies of soil moisture and ST need to be analyzed together using reanalysis data or numerical model.

Data Availability Statement

The monthly station data in this manuscript is from the China National Stations' Fundamental Elements Data sets V3.0 (National Meteorological Information, 2019), which can be obtained from: http://data.tpdc.ac.cn/en/data/52c77e9c-df4a-4e27-8e97-d363fdfce10a/, and is also available at http://101.200.76.197/en/?r=data/detail%26dataCode=SURF_CLI_CHN_MUL_DAY_CES_V3.0. The observation data at Tongyu site is from the Coordinated Energy and Water Cycle Observations Project (CEOP), which has been quality controlled by Tamagawa et al. (2008) and is available at https://archive.eol.ucar.edu/projects/ceop/dm/insitu/sites/ceop_ap/Tongyu/Grassland/.

Acknowledgments
This work was supported by the National Natural Science Foundation of China (Grant 42130609, 41975081, and 41005047), the CAS "Light of West China" Program (E12903010, Y929641001), the Jiangsu University "Blue Project" outstanding young teachers training object, the Fundamental Research Funds for the Central Universities and the Jiangsu Collaborative Innovation Center for Climate Change. The authors show our deepest respect and appreciation to the three anonymous reviewers for their insightful and constructive suggestions to help us largely improve the manuscript.

References

Brunke, M. A., Broxton, P., Pelletier, J., Gochis, D., Hazenberg, P., Lawrence, D. M., et al. (2016). Implementing and evaluating variable soil thickness in the Community Land Model, Version 4.5 (CLM4.5). *Journal of Climate*, *29*(9), 3441–3461. https://doi.org/10.1175/JCLI-D-15-0307.1

Ceccon, C., Panzacchi, P., Scandellari, F., Prandi, L., Ventura, M., Russo, B., et al. (2011). Spatial and temporal effects of soil temperature and moisture and the relation to fine root density on root and soil respiration in a mature apple orchard. *Plant and Soil*, *342*(1–2), 195–206. https://doi.org/10.1007/s11104-010-0684-8

Chen, X., Li, Y., Chau, H. W., Zhao, H., Li, M., Lei, T., & Zou, Y. (2020). The spatiotemporal variations of soil water content and soil temperature and the influences of precipitation and air temperature at the daily, monthly, and annual timescales in China. *Theoretical and Applied Climatology*, *140*(1), 429–451. https://doi.org/10.1007/s00704-020-03092-9

Fan, X. (2009). Impacts of soil heating condition on precipitation simulations in the Weather Research and Forecasting model. *Monthly Weather Review*,*137*, 2263–2285. https://doi.org/10.1175/2009MWR2684.1

García-Suárez, A. M., & Butler, C. J. (2006). Soil temperatures at Armagh observatory, Northern Ireland, from 1904 to 2002. *International Journal of Climatology*, *26*, 1075–1089. https://doi.org/10.1002/joc.1294

Gómez, I., Caselles, V., Estrela, M. J., & Niclòs, R. (2016). Impact of initial soil temperature derived from remote sensing and numerical weather prediction data sets on the simulation of extreme heat events. *Remote Sensing*, *8*(7), 589. https://doi.org/10.3390/rs8070589

Guo, D., Wang, A., Li, D., & Hua, W. (2018). Simulation of changes in the near-surface soil freeze/thaw cycle using CLM4.5 with four atmospheric forcing data sets. *Journal of Geophysical Research: Atmospheres*, *123*, 2509–2523. https://doi.org/10.1002/2017JD028097

Helama, S., Tuomenvirta, H., & Venäläinen, A. (2011). Boreal and subarctic soils under climatic change. *Global and Planetary Change*, *79*, 37–47. https://doi.org/10.1016/j.gloplacha.2011.08.001

Hu, H., Wang, G., Liu, G., Li, T., Ren, D., Wang, Y., et al. (2009). Influences of alpine ecosystem degradation on soil temperature in the freezing-thawing process on Qinghai-Tibet Plateau. *Environmental Geology*, *57*, 1391–1397. https://doi.org/10.1007/s00254-008-1417-7

Hu, Q., & Feng, S. (2004). Why has the land memory changed? *Journal of Climate*, *17*(16), 3236–3243. https://doi.org/10.1175/1520-0442(2004)017<3236:WHTLMC>2.0.CO;2

Iijima, Y., Fedorov, A. N., Park, H., Suzuki, K., Yabuki, H., Maximov, T. C., & Ohata, T. (2010). Abrupt increases in soil temperatures following increased precipitation in a permafrost region, central Lena River basin, Russia Permafrost. *Periglacial Processes*, *21*(1), 30–41. https://doi.org/10.1002/ppp.662

Kang, S., Kim, S., Oh, S., & Lee, D. (2000). Predicting spatial and temporal patterns of soil temperature based on topography, surface cover, and air temperature. *Forest Ecology and Management*, *136*, 173–184. https://doi.org/10.1016/s0378-1127(99)00290-x

Kumar, S., Newman, M., Wang, Y., & Livneh, B. (2019). Potential Reemergence of Seasonal Soil Moisture Anomalies in North America. *Journal of Climate*, *32*(10), 2707–2734. https://doi.org/10.1175/JCLI-D-18-0540.1

Liu, D., & Mishra, A. K. (2017). Performance of AMSR_E soil moisture data assimilation in CLM4.5 model for monitoring hydrologic fluxes at global scale. *Journal of Hydrology*, *547*, 67–79. https://doi.org/10.1016/j.jhydrol.2017.01.036

Liu, Y., & Avissar, R. (1999). A study of persistence in the land-atmosphere system with a fourth-order analytical model. *Journal of Climate*, *12*(8), 2154–2168. https://doi.org/10.1175/1520-0442(1999)012<2154:asopit>2.0.co;2

Ma, Z. (1995). A preliminary analysis for the relationship between the anomalies of soil temperature and either of floods in the Yangtse-Huai river reaches and strong drought in south of Yangtse river in summer of 1991. *Plateau Meteorology*, *14*(2), 185–190. (in Chinese).

Mahanama, S. P. P., Koster, R. D., Reichle, R. H., & Suarez, M. J. (2008). Impact of subsurface temperature variability on surface air temperature variability: An AGCM study. *Journal of Hydrometeorology*, *9*(4), 804–815. https://doi.org/10.1175/2008JHM949.1

Matsumura, S., & Yamazaki, K. (2012). A longer climate memory carried by soil freeze-thaw processes in Siberia. *Environmental Research Letters*, *7*(4), 045402. https://doi.org/10.1088/1748-9326/7/4/045402

Mihalakakou, G., Santamouris, M., Lewis, J. O., & Asimakopoulos, D. N. (1997). On the application of the energy balance equation to predict ground temperature profiles. *Solar Energy*, *60*(3–4), 181–190. https://doi.org/10.1016/s0038-092x(97)00012-1

National Meteorological Information Center. (2019). Daily meteorological data set of basic meteorological elements of China National Surface Weather Station (V3.0) [Dataset]. National Tibetan Plateau Data Center. Retrieved from http://data.tpdc.ac.cn/en/data/52c77e9c-df4a-4e27-8e97-d363fdfce10a/

Oleson, K., Lawrence, D. M., Bonan, G. B., Drewniak, B., Huang, M., Koven, C. D., et al. (2013). Technical description of version 4.5 of the Community Land Model (CLM). In *NCAR Technical Note NCAR/TN-503+STR* (p. 434). National Center for Atmospheric Research.

Qian, B., Gregorich, E. G., Gameda, S., Hopkins, D. W., & Wang, X. L. (2011). Observed soil temperature trends associated with climate change in Canada. *Journal of Geophysical Research*, *116*, D0216. https://doi.org/10.1029/2010jd015012

Schaefer, K. M., Zhang, T., Tans, P. P., & Stöckli, R. (2007). Temperature anomaly reemergence in seasonally frozen soils. *Journal of Geophysical Research*, *112*, D20102. https://doi.org/10.1029/2007JD008630

Song, Y. M., Fan, Y., & Ma, T. J. (2014). Evaluation of simulation performance of land surface model NCAR_CLM4.5 at a degrated glassland station in semi-arid area. *Transactions of Atmospheric Sciences*, *7*(6), 794–803. (in Chinese).

Song, Y. M., Huang, A. N., & Chen, H. S. (2022). The storage of antecedent precipitation and air temperature signals in soil temperature over China. *Journal of Hydrometeorology*, *23*(3), 377–388. https://doi.org/10.1175/JHM-D-21-0126.1

Tamagawa, K., Kitsuregawa, M., Ikoma, E., Ohta, T., Williams, S., & Koike, T. (2008). An advanced quality control system for the CEOP/CAMP in situ data management. *IEEE Systems Journal*, *2*(3), 406–413. https://doi.org/10.1109/jsyst.2008.927710

Tang, M., Wang, J., & Zhang, J. (1987). A primary method for predicting the spring rainfall by the winter soil temperature depth 80 cm. *Plateau Meteorology*, *6*(3), 244–255. (in Chinese).

Tesař, M., Šír, M., Krejča, M., & Váchal, J. (2008). Influence of vegetation cover on air and soil temperatures in the Šumava Mts. (Czech Republic). *IOP Conference Series: Earth and Environmental Science*, *4*, 012029. https://doi.org/10.1088/1755-1307/4/1/012029

Wang, A., Zeng, X., & Guo, D. (2016). Estimates of global surface hydrology and heat fluxes from the Community Land Model (CLM4.5) with four atmospheric forcing data sets. *Journal of Hydrometeorology*, *17*(9), 2493–2510. https://doi.org/10.1175/JHM-D-16-0041.1

Wang, Y. H., Chen, W., Zhang, J. Y., & Nath, D. (2013). Relationship between soil temperature in May over Northwest China and the East Asian summer monsoon precipitation. *Acta Meteorologica Sinica*, *27*(5), 716–724. https://doi.org/10.1007/s13351-013-0505-0

Wu, L., & Zhang, J. (2014). Strong subsurface soil temperature feedbacks on summer climate variability over the arid/semi-arid regions of East Asia. *Atmospheric Science Letters*, *15*(4), 307–313. https://doi.org/10.1002/asl2.504

Wundram, D., Pape, R., & Löffler, J. (2010). Alpine soil temperature variability at multiple scales. *Arctic, Antarctic, and Alpine Research*, *42*(1), 117–128. https://doi.org/10.1657/1938-4246-42.1.117

Xue, Y., Diallo, I., Li, W., Neelin, J. D., Chu, P. C., Vasic, R., et al. (2018). Spring land surface and subsurface temperature anomalies and subsequent downstream late spring-summer drought/floods in North America and East Asia. *Journal of Geophysical Research: Atmospheres*, *123*(10), 5001–5019. https://doi.org/10.1029/2017jd028246

Yang, K., & Zhang, J. (2016). Spatiotemporal characteristics of soil temperature memory in China from observation. *Theoretical and Applied Climatology*, *126*(3–4), 739–749. https://doi.org/10.1007/s00704-015-1613-9

Yang, Y., Wu, Z., He, H., Du, H., Wang, L., Guo, X., & Zhao, W. (2018). Differences of the changes in soil temperature of cold and mid-temperate zones, northeast China. *Theoretical and Applied Climatology*, *134*(1–2), 633–643. https://doi.org/10.1007/s00704-017-2297-0

Zhang, H. X., Yuan, N. M., Ma, Z. G., & Huang, Y. (2021). Understanding the soil temperature variability at different depths: Effects of surface air temperature, snow cover, and the soil memory. *Advances in Atmospheric Sciences*, *38*(3), 493–503. https://doi.org/10.1007/s00376-020-0074-y

Zhang, S. Y., & Li, X. Y. (2018). Soil moisture and temperature dynamics in typical alpine ecosystems: A continuous multi-depth measurements-based analysis from the Qinghai-Tibet plateau, China. *Hydrology Researc*h, *49*(1), 194–209. https://doi.org/10.2166/nh.2017.215